



**RESEARCH REPORT**

VTT-R-00796-18 | 14.2.2018

# Shielding analysis of a spent fuel storage cask using variance reduction with Serpent

Author: Silja Häkkinen

Confidentiality: Public



<b>Report's title</b> Shielding analysis of a spent fuel storage cask using variance reduction with Serpent		
<b>Customer, contact person, address</b> VYR		<b>Order reference</b> SAFIR2018
<b>Project name</b> Nuclear Criticality Safety Analyses Preparedness at VTT		<b>Project number/Short name</b> 113443 — SAFIR2018/KATVE
<b>Author</b> Silja Häkkinen		<b>Pages</b> 15
<b>Keywords</b> Serpent, variance reduction, weight windows		<b>Report identification code</b> VTT-R-00796-18
<p><b>Summary</b></p> <p>Variance reduction routines are often employed when making particle transport calculations with Monte Carlo codes in a geometry involving regions of very low particle density. This improves the statistical accuracy of the calculation and reduces the calculation time. Shielding calculations are a type of particle transport calculation where the particle density is intentionally kept low in the regions of interest and the use of variance reduction is profitable.</p> <p>Recently, variance reduction techniques in the form of weight windows have been implemented in VTT's Monte Carlo code Serpent. In this work, Serpent's variance reduction methods have been tested by calculating photon dose rate and neutron flux on the surface of a castor storage cask in air. The cask was filled with burned UO<sub>2</sub> or MOX assemblies and the figure of merit, FOM, of calculations with and without variance reduction was compared.</p> <p>Variance reduction improved FOM in the photon transport calculations by several orders of magnitude compared to calculations without variance reduction. In the neutron transport calculations, FOM was approximately 3 times higher with variance reduction than without it. This is because the castor storage cask absorbs neutrons far less effectively than photons. The calculated photon dose rates and neutron flux with variance reduction corresponded to the values calculated without variance reduction within relative standard deviation in most cases. In the cases where the two values differed from each other, it was concluded to be caused mainly by the poor statistics of the calculations without variance reduction. Some of these cases without variance reduction were calculated with a larger number of particle histories and the differences vanished.</p>		
<b>Confidentiality</b>		Public
Espoo, 14.2.2018		
<b>Written by</b>	<b>Reviewed by</b>	<b>Accepted by</b>
Silja Häkkinen, Research Scientist	Jaakko Leppänen, Research Professor	Petri Kotiluoto, Research Team Leader
<b>VTT's contact address</b> P.O. Box 1000, Vuorimiehentie 3, 02044 VTT, Espoo, Finland		
<b>Distribution (customer and VTT)</b> VTT Oy SAFIR RG3		
<p><i>The use of the name of VTT Technical Research Centre of Finland Ltd in advertising or publishing of a part of this report is only permissible with written authorisation from VTT Technical Research Centre of Finland Ltd.</i></p>		

## Contents

---

<b>1 Description and Objectives .....</b>	<b>3</b>
<b>2 Model .....</b>	<b>3</b>
2.1 Fuel Assemblies.....	4
2.2 Castor Storage Cask .....	5
<b>3 Methods .....</b>	<b>6</b>
3.1 Serpent .....	6
3.2 Weight Window Mesh Generation.....	7
3.3 Calculation cases .....	7
<b>4 Results .....</b>	<b>9</b>
<b>5 Conclusions .....</b>	<b>10</b>
<b>6 Summary .....</b>	<b>10</b>
<b>References .....</b>	<b>11</b>

## 1 Description and Objectives

---

VTT has a long history in development of calculation codes related to various parts of nuclear power plant simulation. One of these codes is Serpent. Serpent is a multi-purpose three-dimensional continuous-energy Monte Carlo transport code developed at VTT since 2004 [1]. The code started as a reactor physics code, but during recent years the capabilities of the current version, Serpent 2, have been extended to multi-physics simulations and neutron and photon transport simulations. Neutron and photon transport simulations are needed e.g. in radiation dose rate calculations and shielding analysis.

In radiation dose rate calculations and shielding analysis, the particle intensity in the region of interest can be rather low. This increases the required calculation time and decreases the statistical accuracy. This kind of problems can be overcome by using variance reduction techniques. The purpose of these techniques is to reduce the variance associated to the output of random variables in a simulation and thus increase the precision of the results. One of the variance reduction techniques is importance sampling. This technique has been recently implemented in Serpent in the form of weight-window generation [2]. The weight-window based approach utilizes an importance mesh overlaid on top of the geometry. The mesh is divided in areas of varying importance. When particles enter a region of higher importance, the particles are split, and when they exit to a lower importance region, some of the particles are terminated by Russian roulette.

The purpose of this work is to test the variance reduction routines implemented in Serpent. This is accomplished by calculating photon dose rates and neutron flux on the surface of a storage cask with and without variance reduction and comparing the resulting figures of merit.

The report is organized as follows. The simulated model including fuel assemblies and storage cask are described in section 2. Changes to Serpent, weight window mesh generation and the calculation cases are introduced in section 3 and the results are listed in section 4. Lastly, conclusions are discussed in section 5 and a brief summary is given in section 6.

## 2 Model

---

The calculation chain in this work includes three steps:

1. Burnup calculation on assembly level in three dimensions.
2. Decay calculation of the burned assembly.
3. Transport calculation modelling a three dimensional castor storage cask that contains 21 similar fuel assemblies.

## 2.1 Fuel Assemblies

Two different EPR 17x17 UOX and MOX fuel assemblies, were modelled. The main parameters related to the geometry of the assemblies are presented in table 1. The MOX assembly is presented in figures 1a and 1b [3,4]. The larger blue rods in the figures represent guide tubes and the instrumentation tube filled with water. The UOX assemblies are similar to the MOX assemblies in figures 1a and 1b except that all fuel rods in the UOX assembly are the same.

**Table 1.** Dimensions of the UOX and MOX fuel assemblies.

Parameter	Value
Fuel radius [cm]	0.39218
Cladding inner radius [cm]	0.40005
Cladding outer radius [cm]	0.45720
Cladding material	Zircaloy
Pin pitch [cm]	1.25984
Assembly pitch [cm]	21.50364
Active fuel length [cm]	365.76
Fuel pins in assembly	264
Guide / Instrument tubes in assembly	24 / 1
UO <sub>2</sub> fuel density [g/cm <sup>3</sup> ]	10.30166
MOX fuel density [g/cm <sup>3</sup> ]	11.3

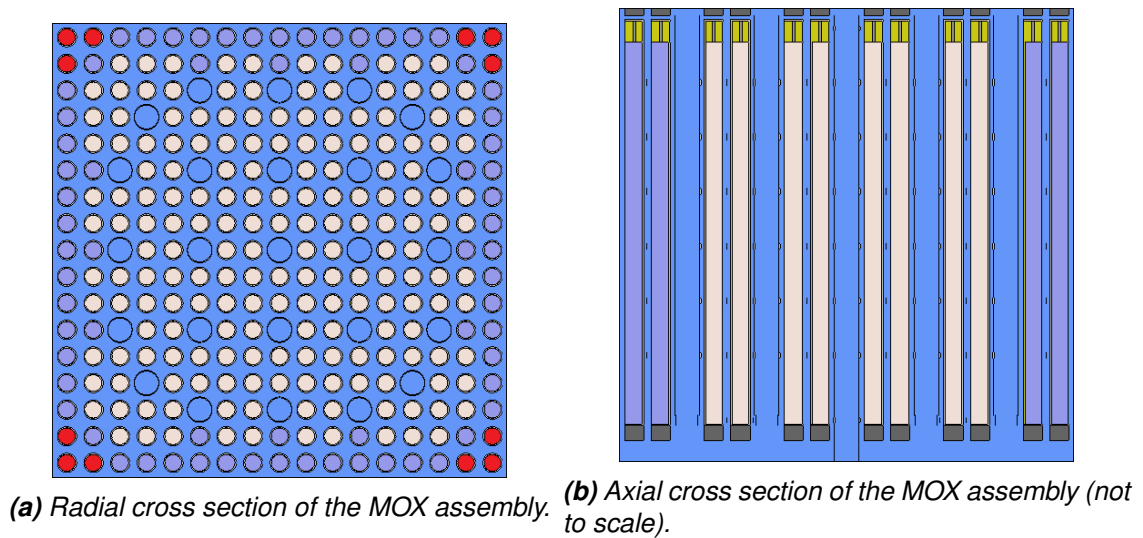


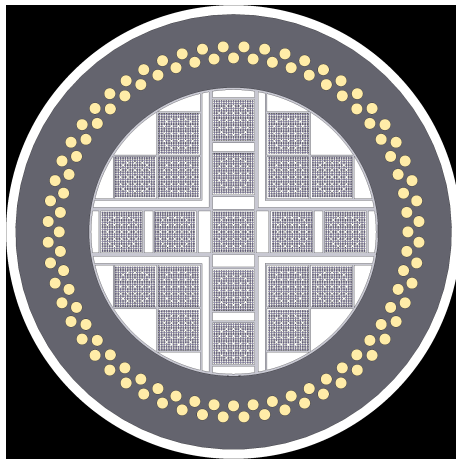
**Figure 1.** The modelled MOX fuel assembly.

The UOX assembly consists of one type of 3.1 % enriched UO<sub>2</sub> fuel [3]. The MOX fuel consists of three types of rods with plutonium content 3.65 %, 6.49 % and 9.77 % of heavy metal [4]. In figure 1a, the red rods in the corners have the lowest plutonium content. The purple rods on the edges of the assembly have the second lowest plutonium content and the rest of the rods are the highest content rods. The mass fraction of oxygen is 11.8 % in all fuel types.

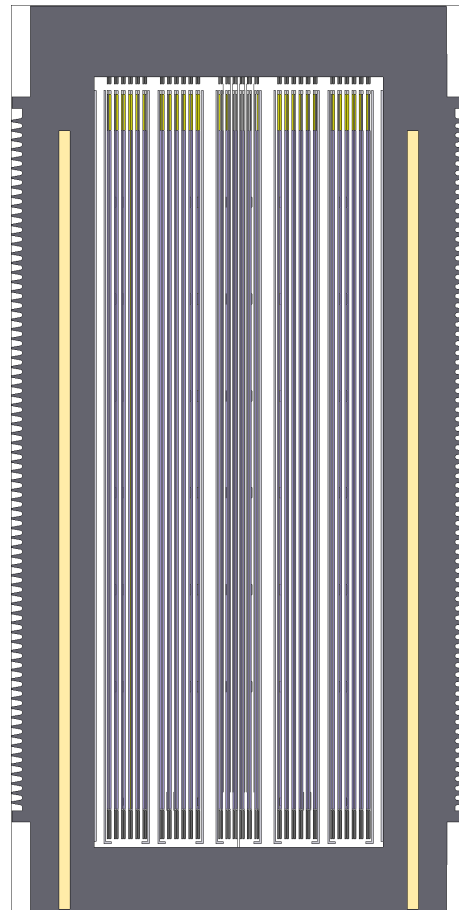
The burnup calculations were performed up to 50 MWd/kgU. The first burnup steps were 0.1, 0.5 and 1.0 MWd/kgU after which the step size was 1 MWd/kgU. Reactor power was set to 17.674 MW. Reflective boundary conditions were used in the radial direction and black boundary conditions in the axial direction. The ENDF/B-VII cross section library was used. In order to model radioactive decay of the burned fuel assemblies, the calculation was restarted on desired burnup points and the fuel was allowed to decay for 100 years.

## 2.2 Castor Storage Cask

For the photon and neutron transport calculations, a castor storage cask was filled with the burned fuel assemblies. The storage cask is presented in figures 2a and 2b. The cask has been modelled using CAD-based geometry type [5]. The light grey grid represents the stainless steel basket holding the fuel assemblies. The yellow tubes in the figures are polyethylene moderator rods designed for neutron moderation. The dark grey areas represent the cast iron cask surrounding the basket. The outer surface of the cask is covered with radial fins designed to improve the passive heat removal.



**(a)** Radial cross section of the castor storage cask.



**(b)** Axial cross section of the castor storage cask (not to scale).

**Figure 2.** Cross sections of the castor storage cask in axial and radial directions.

## 3 Methods

---

### 3.1 Serpent

Variance reduction is available in the current update of Serpent, Version 2.1.29. The syntax is such that firsts an importance map is calculated using the "wwgen" card and then, the generated importance map is applied in the transport calculations using the "wwin" card. The wwgen card generates an importance mesh with user defined boundaries. The mesh can be either cartesian or cylindrical and it can be divided in equidistant segments in all three dimensions. More information on the use of these cards can be found in Serpent Wiki [6]

In order to successfully complete the calculations required for this work, some changes were needed in the source code that are not yet available in the published version 2.1.29. These changes are listed here.

- Due to the strong shielding effect of the castor storage cask, the amount of particles, especially photons, reaching the edges and corners of the cask was considerably lower than in the centre of the cask. On the other hand, the task was to calculate the radiation dose on the outer surface of the cask. With an equally spaced mesh, it was difficult to get sufficiently high importances on the edges and corners of the cask. In order to get a properly functioning importance mesh, the mesh needed to be denser near the edges and sparser in the middle. For this reason, the variance reduction routine of Serpent was updated to include a cylindrical mesh with the possibility for unequal mesh spacing.
- The task was to calculate photon dose rate through the storage cask surface but there was no suitable detector in Serpent for this purpose. The closest was the Surface current detector that calculates the particle current through a given surface. However, the detector does not allow responses that would determine the calculation of dose rate. The problem was solved by introducing a Surface flux detector in Serpent.

A couple of bugs were also found in Serpent that were corrected during the work:

- There was a bug in the Serpent subroutine "pairproduction.c" causing some simulations to get stuck in a transport calculation using a photon detector.
- A bug was found in the Serpent subroutine "readrestartfile.c" that is used to restart a burnup or a decay calculation. The bug was related to using the index of a burnup or decay step. Index number 0 and 1 were both pointing to the zero burnup or decay step. The bug was corrected so that index 0 ("set rfr idx 0") points to the zero burnup or decay step and index 1 points to the first burnup or decay step.

### 3.2 Weight Window Mesh Generation

In order to get enough particles on the edges and corners of the storage cask, two importance meshes were generated for the photon transport calculations. The first mesh was generated with a sparser mesh in order to get sufficient statistics everywhere in the geometry. The mesh was generated using 10 MeV source particles. The second mesh applied the burned fuel as the source [7] and it was generated using the first mesh for variance reduction in order to emphasize the edges. The division of the meshes in each direction is given in table 2 for both meshes.

**Table 2.** Division of the importance meshes. In the table,  $r$  denotes the number of circular radial segments,  $\theta$  denotes the number of angular sections and  $z$  denotes the number of axial segments.

Mesh	$r$	$\theta$	$z$
Mesh 1	11	1	25
Mesh 2	37	1	63

In mesh 1, the active length of the fuel was divided in five axial segments of 73.2 cm and the regions above and below the active fuel were divided in ten segments of 6.72 cm (above) and 5.60 cm (below). Radially, the basket inside the iron cask containing the fuel assemblies comprised one segment of 74.0 cm and the rest of the cask was divided in ten segments of 4.61 cm. Mesh 2 had a considerably denser division. The active length of the fuel was divided in 20 axial segments of 18.3 cm, the regions above were divided in 23 axial segments of 2.92 cm and the regions below in 20 axial segments of 2.80 cm. Radially, the basket was divided in 15 segments of 4.93 cm and the rest of the cask was divided in 22 segments of 2.10 cm. For the neutron transport calculations, only one mesh was used (mesh 2), since neutrons penetrate more easily through the cask and one mesh was enough.

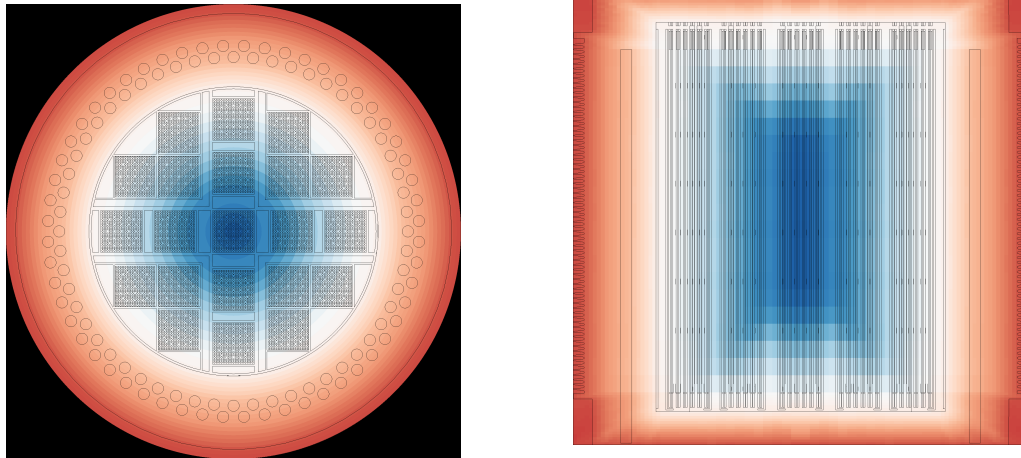
Figures 3a and 3b give an example of the generated importance meshes on top of the modelled geometry for the UOX assemblies in photon transport calculations. In the MOX case, it was difficult to get enough particles in the top corners of the cask and a small circular ring of diameter 2.1 cm and 2.92 cm in height was not included in the final mesh. However, the effect on the final results was considered negligible due to the small size of the ring and its location at the top corners where the particle flux is low.

### 3.3 Calculation cases

The goal of the work was to test the efficiency of the variance reduction routine in Serpent. This was accomplished by calculating the photon dose rate and neutron flux on the surface of the castor storage cask with and without variance reduction and comparing the respective figures of merit, FOM. FOM is defined by equation 1

$$\text{FOM} = \frac{1}{\sigma^2 T}, \quad (1)$$





(a) Radial cross section of the importance mesh. (b) Axial cross section of the importance mesh (not to scale).

**Figure 3.** Importance mesh covering the storage cask generated for the UOX assemblies in photon transport calculations. Red colour indicates high importance and blue color low importance. White denotes importance 1.

where  $\sigma$  is the standard deviation of the photon dose rate (or neutron flux) and  $T$  is the wall-clock running time of the transport calculation in hours.

The FOM of the photon dose rate and neutron flux calculations was determined at two burnup steps, 20 MWd/kgU and 50 MWd/kgU, and five different decay times, 0, 10, 30, 50 and 100 years for both studied fuel types, UO<sub>2</sub> and MOX. The weight window meshes were generated separately for each case (fuel, burnup, transport particle), but not separately for every decay time. All meshes were generated using 0 decay time for the burned fuel. This was done in the interest to save time. It was assumed a justified approximation because the energy spectrum of the source, and therefore the obtained importance mesh, is not expected to change drastically during 100 years even though the intensity of the source will decrease significantly. The assumption was tested by generating a couple of meshes with different decay times and using these meshes in the transport calculations at the corresponding decay time. The resulting dose rates agreed with the dose rates calculated using the mesh generated at 0 decay time. The number of source particles used in the importance mesh generation and in the transport calculations is given in table 3.

**Table 3.** Number of source particles in the calculations. The value in the brackets indicates transport calculation after 100 years cooling time.

	UOX photon	MOX photon	UOX neutron	MOX neutron
Mesh 1	$3 \cdot 10^8$	$3 \cdot 10^8$	—	—
Mesh 2	$1 \cdot 10^8$	$5 \cdot 10^8$	$1 \cdot 10^7$	$1 \cdot 10^7$
Transport calc	$2 \cdot 10^8$ ( $5 \cdot 10^8$ )	$2 \cdot 10^8$ ( $5 \cdot 10^8$ )	$2 \cdot 10^7$	$2 \cdot 10^7$
No var. reduc.	$2 \cdot 10^{10}$ ( $3 \cdot 10^{10}$ )	$2 \cdot 10^{10}$ ( $3 \cdot 10^{10}$ )	$1 \cdot 10^8$	$1 \cdot 10^8$

All calculations have been made in VTT's Linux cluster Potku2, espnr130.ad.vtt.fi. The

calculations were run on similar 28-core 2.60 GHz Intel Xeon cluster nodes using 7 cores in all cases. Every transport calculation with the same cooling time was run on the exact same node. The calculations can be found under the directory [espn130.ad.vtt.fi/~home/shsilja/SAFIR/KATVE/DryStorage/](http://espn130.ad.vtt.fi/~home/shsilja/SAFIR/KATVE/DryStorage/).

## 4 Results

The calculation time of the importance mesh generation in hours is given in table 4.

**Table 4.** Calculation time of the importance meshes in hours. The value on the upper row for mesh 2 indicates the calculation time at 20 MWd/kgU fuel burnup and the value on the bottom row 50 MWd/kgU fuel burnup.

	UOX photon	MOX photon	UOX neutron	MOX neutron
Mesh 1	6.04	6.66	–	–
Mesh 2	0.517	2.64	1.75	2.34
	0.478	2.62	1.65	1.92

The total calculation time and the results of all calculations are presented in tables 5 and 6. For the cases using variance reduction, the total calculation time is a sum of the time taken to generate the importance meshes and the time taken to complete the transport calculations. In the tables, the results are given for each calculated assembly and transport particle type combination with and without variance reduction. Four values are given for each case from top to bottom: photon dose rate or neutron flux, the associated relative standard deviation in brackets, the total calculation time in hours and the figure of merit, FOM. The photon dose rates (neutron flux) in red indicate that the results with and without variance reduction do not agree within the relative standard deviation.

Some of the calculated dose rates (neutron flux) with variance reduction do not agree with the dose rates (neutron flux) without variance reduction as indicated in red in tables 5 and 6. The reason for the deviations is probably poor statistics in the calculations without variance reduction. This assumption was tested by repeating some of the calculations using more source particles,  $5 \cdot 10^{10}$  in photon dose rate calculations and  $3 \cdot 10^8$  in neutron flux calculations. In all cases the new result agreed with the corresponding result with variance reduction.

The increase in source particles somewhat improved the statistics of the calculation by decreasing the standard deviation to less than half of the original value. Nevertheless, the statistics in the photon dose rate calculations without variance reduction remained very poor. Also, the calculation time multiplied in proportion to the increase in the source particles which made simply increasing the number of source particles a very ineffective way of improving the statistics of the calculations.

The figure of merit, FOM, presented in the tables 5 and 6 is also presented in figures 4 (photon dose rate) and 5 (neutron flux). The difference in the respective FOMs with and without variance reduction is evident in the figures. The difference is especially pronounced in the case of photon dose rate since the storage cask absorbs gamma

radiation considerably more effectively than neutrons.

## 5 Conclusions

---

It can be seen in tables 5 and 6 that the calculation times are 3 - 13 times longer without variance reduction than with variance reduction. The statistics of the calculations is also worse without variance reduction, especially in the photon dose rate calculations. For example, the standard deviation of the photon transport calculation without variance reduction for the MOX case after 30 years of decay was 0.289 and the calculation time was about three days. Multiplying the number of source particles by 2.5 decreases the standard deviation to 0.117 which is still very bad and the calculation time is increased to a full week. It is clear that improving the statistics of the photon transport calculations by increasing the number of particles is very impractical and time consuming. However, employing variance reduction in Serpent considerably improves the statistics and reduces the calculation time.

In this example, it seems that calculation of the neutron flux is feasible also without variance reduction. The statistics of the calculations is rather good and the calculation times remain reasonable. Even so, variance reduction can clearly reduce the calculation time without any cost to the good statistics of the results.

## 6 Summary

---

In this work, the newly implemented variance reduction routines of VTT's Monte Carlo code Serpent have been tested. Photon dose rate and neutron flux was calculated on the surface of a castor storage cask filled with burned  $\text{UO}_2$  or MOX assemblies. The figure of merit, FOM, of calculations employing variance reduction was compared to the corresponding FOM without variance reduction. The calculations were repeated for two burnup values, 20 and 50 MWd/kgU, and several decay times from 0 to 100 years. In the photon transport calculations, for both types of fuel the employment of variance reduction increased FOM several orders of magnitude compared to calculations without variance reduction. For neutron transport calculations, FOM was also improved (a few hundred percent) but the effect was considerably less pronounced. Also for neutron flux, the calculation time remained reasonable (less than a day) even without variance reduction. This is because the storage cask in air absorbs neutrons considerably less effectively than photons.

The photon dose rates and neutron flux calculated using variance reduction corresponded to the values calculated without variance reduction within the relative standard deviation in most cases. In some cases there were differences. These differences seem to arise mainly from poor statistics, especially in the calculations without variance reduction. Some of the calculations without variance reduction were repeated using more particle histories in order to improve the statistical accuracy. In every calculated case with larger number of particle histories, the differences between calculations with and without vari-

ance reduction disappeared. Thus, it can be concluded that the newly developed variance reduction routine in Serpent is functioning and it is capable of improving the statistics and effectiveness of particle transport calculations in shielding calculations.

## References

---

- [1] J. Leppänen et al., "The Serpent Monte Carlo code: Status, development and applications in 2013", *Ann. Nucl. Energy*, 82, p. 142-150, 2015.
- [2] J. Leppänen et al., "Development of Variance Reduction Scheme in the Serpent 2 Monte Carlo Code", *M&C 2017 - International Conference on Mathematics & Computational Methods Applied to Nuclear Science & Engineering*, Korea, April 16-20, 2017.
- [3] N. Horelik et al., "Benchmark for Evaluation and Validation of Reactor Simulations", rev. 2.0, MIT Computational Reactor Physics Group, October 2016.
- [4] R. Eschbach et al., "Proposal for a Benchmark on Dose Rate Calculations for Irradiated Assemblies by the WPFC/AFCS Expert Group", October 2015.
- [5] J. Leppänen, "CAD-based Geometry Type in Serpent 2 – Application in Fusion Neutronics." In *proc. M&C + SNA + MC 2015 Nashville, TN, Apr. 19-23, 2015*.
- [6] "Serpent Wiki", [http://serpent.vtt.fi/mediawiki/index.php/Main\\_Page](http://serpent.vtt.fi/mediawiki/index.php/Main_Page)
- [7] J. Leppänen and T. Kaltiaisenaho, "Expanding the Use of Serpent 2 to Fusion Applications: Shut-down Dose Rate Calculations." In *proc. PHYSOR 2016, Sun Valley, ID, May 1-6, 2016*.

**Table 5.** Results with burnup 20 MWd/kgU. For each assembly and particle type, four values are given in the table. From top to bottom these are: photon dose rate (or neutron flux for neutrons), associated relative standard deviation, total calculation time, figure of merit, FOM. The blue rows indicate calculations without variance reduction and the white rows with variance reduction. The values in red indicate deviation between the result with variance reduction and the result without variance reduction that is not accounted for by standard deviation.

Decay time [y]:	0	10	30	50	100
UOX photon	$5.27 \cdot 10^{13}$	$7.99 \cdot 10^7$	$1.97 \cdot 10^7$	$1.01 \cdot 10^7$	$2.16 \cdot 10^6$
	(0.01046)	(0.13097)	(0.19088)	(0.2126)	(0.17044)
	77	92	89	87	194
UOX photon	$1.19 \cdot 10^2$	$6.36 \cdot 10^{-1}$	$3.09 \cdot 10^{-1}$	$2.55 \cdot 10^{-1}$	$1.77 \cdot 10^{-1}$
	$5.28 \cdot 10^{13}$	$9.32 \cdot 10^7$	$2.29 \cdot 10^7$	$1.01 \cdot 10^7$	$2.59 \cdot 10^6$
	(0.00373)	(0.00666)	(0.0076)	(0.0079)	(0.00452)
MOX photon	13	12	10	10	15
	$5.52 \cdot 10^3$	$1.92 \cdot 10^3$	$1.68 \cdot 10^3$	$1.58 \cdot 10^3$	$3.32 \cdot 10^3$
	$4.04 \cdot 10^{13}$	$4.76 \cdot 10^8$	$6.13 \cdot 10^7$	$2.54 \cdot 10^7$	$3.07 \cdot 10^6$
MOX photon	(0.01269)	(0.10751)	(0.28947)	(0.31933)	(0.74342)
	78	79	69	61	72
	$7.99 \cdot 10^1$	$1.09 \cdot 10^0$	$1.74 \cdot 10^{-1}$	$1.60 \cdot 10^{-1}$	$2.53 \cdot 10^{-2}$
MOX photon	$4.02 \cdot 10^{13}$	$4.32 \cdot 10^8$	$1.02 \cdot 10^8$	$3.39 \cdot 10^7$	$7.12 \cdot 10^6$
	(0.00399)	(0.00979)	(0.01307)	(0.01463)	(0.01082)
	14	13	12	12	14
UOX neutron	$4.44 \cdot 10^3$	$7.87 \cdot 10^2$	$4.97 \cdot 10^2$	$4.06 \cdot 10^2$	$6.26 \cdot 10^2$
	$1.65 \cdot 10^{14}$	$4.98 \cdot 10^5$	$2.55 \cdot 10^5$	$1.43 \cdot 10^5$	$5.88 \cdot 10^4$
	(0.0011)	(0.00078)	(0.00076)	(0.00076)	(0.00079)
UOX neutron	16	19	18	18	18
	$5.13 \cdot 10^4$	$8.84 \cdot 10^4$	$9.67 \cdot 10^4$	$9.67 \cdot 10^4$	$8.85 \cdot 10^4$
	$1.65 \cdot 10^{14}$	$4.99 \cdot 10^5$	$2.56 \cdot 10^5$	$1.43 \cdot 10^5$	$5.88 \cdot 10^4$
MOX neutron	(0.00099)	(0.00072)	(0.00068)	(0.00065)	(0.0007)
	5.4	6.3	6.1	6.1	6.0
	$1.88 \cdot 10^5$	$3.04 \cdot 10^5$	$3.56 \cdot 10^5$	$3.89 \cdot 10^5$	$3.38 \cdot 10^5$
MOX neutron	$2.54 \cdot 10^{14}$	$2.22 \cdot 10^8$	$1.02 \cdot 10^8$	$4.82 \cdot 10^7$	$1.02 \cdot 10^7$
	(0.00135)	(0.0007)	(0.01033)	(0.00119)	(0.00073)
	21	23	22	21	21
MOX neutron	$2.60 \cdot 10^4$	$8.99 \cdot 10^4$	$4.26 \cdot 10^2$	$3.33 \cdot 10^4$	$9.07 \cdot 10^4$
	$2.54 \cdot 10^{14}$	$2.22 \cdot 10^8$	$1.01 \cdot 10^8$	$4.82 \cdot 10^7$	$1.03 \cdot 10^7$
	(0.00099)	(0.0008)	(0.00084)	(0.0009)	(0.00071)
MOX neutron	6.8	7.5	7.0	7.1	7.0
	$1.50 \cdot 10^5$	$2.08 \cdot 10^5$	$2.02 \cdot 10^5$	$1.75 \cdot 10^5$	$2.84 \cdot 10^5$

**Table 6.** Results with burnup 50 MWd/kgU. For each assembly and particle type, four values are given in the table. From top to bottom these are: photon dose rate (or neutron flux for neutrons), associated relative standard deviation, total calculation time, figure of merit, FOM. The blue rows indicate calculations without variance reduction and the white rows with variance reduction. The values in red indicate deviation between the result with variance reduction and the result without variance reduction that is not accounted for by standard deviation.

Decay time [y]:	0	10	30	50	100
UOX photon	$4.74 \cdot 10^{13}$	$4.02 \cdot 10^8$	$7.94 \cdot 10^7$	$4.12 \cdot 10^7$	$4.20 \cdot 10^6$
	(0.01233)	(0.11156)	(0.1497)	(0.17446)	(0.23014)
	72	93	88	86	121
UOX photon	$9.11 \cdot 10^1$	$8.63 \cdot 10^{-1}$	$5.05 \cdot 10^{-1}$	$3.84 \cdot 10^{-1}$	$1.56 \cdot 10^{-1}$
	$4.67 \cdot 10^{13}$	$3.68 \cdot 10^8$	$7.53 \cdot 10^7$	$2.84 \cdot 10^7$	$6.48 \cdot 10^6$
	(0.00427)	(0.00556)	(0.00795)	(0.00704)	(0.00415)
MOX photon	13	12	10	10	15
	$4.21 \cdot 10^3$	$2.67 \cdot 10^3$	$1.51 \cdot 10^3$	$1.93 \cdot 10^3$	$3.75 \cdot 10^3$
	$4.08 \cdot 10^{13}$	$1.54 \cdot 10^9$	$3.19 \cdot 10^8$	$1.27 \cdot 10^8$	$2.08 \cdot 10^7$
MOX photon	(0.01262)	(0.0941)	(0.14357)	(0.2646)	(0.25944)
	77	84	77	72	88
	$8.15 \cdot 10^1$	$1.35 \cdot 10^0$	$6.34 \cdot 10^{-1}$	$1.99 \cdot 10^{-1}$	$1.69 \cdot 10^{-1}$
MOX photon	$4.04 \cdot 10^{13}$	$1.45 \cdot 10^9$	$3.19 \cdot 10^8$	$9.81 \cdot 10^7$	$1.74 \cdot 10^7$
	(0.00432)	(0.00971)	(0.00999)	(0.01158)	(0.00924)
	14	14	12	12	15
UOX neutron	$3.81 \cdot 10^3$	$7.86 \cdot 10^2$	$8.34 \cdot 10^2$	$6.30 \cdot 10^2$	$8.07 \cdot 10^2$
	$1.27 \cdot 10^{14}$	$2.95 \cdot 10^7$	$1.39 \cdot 10^7$	$6.76 \cdot 10^6$	$1.46 \cdot 10^6$
	(0.00124)	(0.00078)	(0.00078)	(0.00077)	(0.001)
UOX neutron	15	17	17	17	17
	$4.31 \cdot 10^4$	$9.45 \cdot 10^4$	$9.73 \cdot 10^4$	$1.00 \cdot 10^5$	$5.95 \cdot 10^4$
	$1.27 \cdot 10^{14}$	$2.95 \cdot 10^7$	$1.39 \cdot 10^7$	$6.75 \cdot 10^6$	$1.46 \cdot 10^6$
MOX neutron	(0.00114)	(0.00066)	(0.00068)	(0.00091)	(0.00069)
	5.2	6.3	5.9	5.8	5.9
	$1.49 \cdot 10^5$	$3.67 \cdot 10^5$	$3.68 \cdot 10^5$	$2.07 \cdot 10^5$	$3.55 \cdot 10^5$
MOX neutron	$1.88 \cdot 10^{14}$	$7.71 \cdot 10^8$	$3.60 \cdot 10^8$	$1.78 \cdot 10^8$	$4.51 \cdot 10^7$
	(0.00109)	(0.00077)	(0.00082)	(0.00078)	(0.00075)
	18	20	19	18	19
MOX neutron	$4.73 \cdot 10^4$	$8.65 \cdot 10^4$	$7.87 \cdot 10^4$	$9.03 \cdot 10^4$	$9.51 \cdot 10^4$
	$1.88 \cdot 10^{14}$	$7.73 \cdot 10^8$	$3.60 \cdot 10^8$	$1.77 \cdot 10^8$	$4.51 \cdot 10^7$
	(0.00102)	(0.00071)	(0.00078)	(0.00076)	(0.00079)
MOX neutron	5.9	6.6	6.3	6.2	6.2
	$1.64 \cdot 10^5$	$3.03 \cdot 10^5$	$2.60 \cdot 10^5$	$2.78 \cdot 10^5$	$2.60 \cdot 10^5$

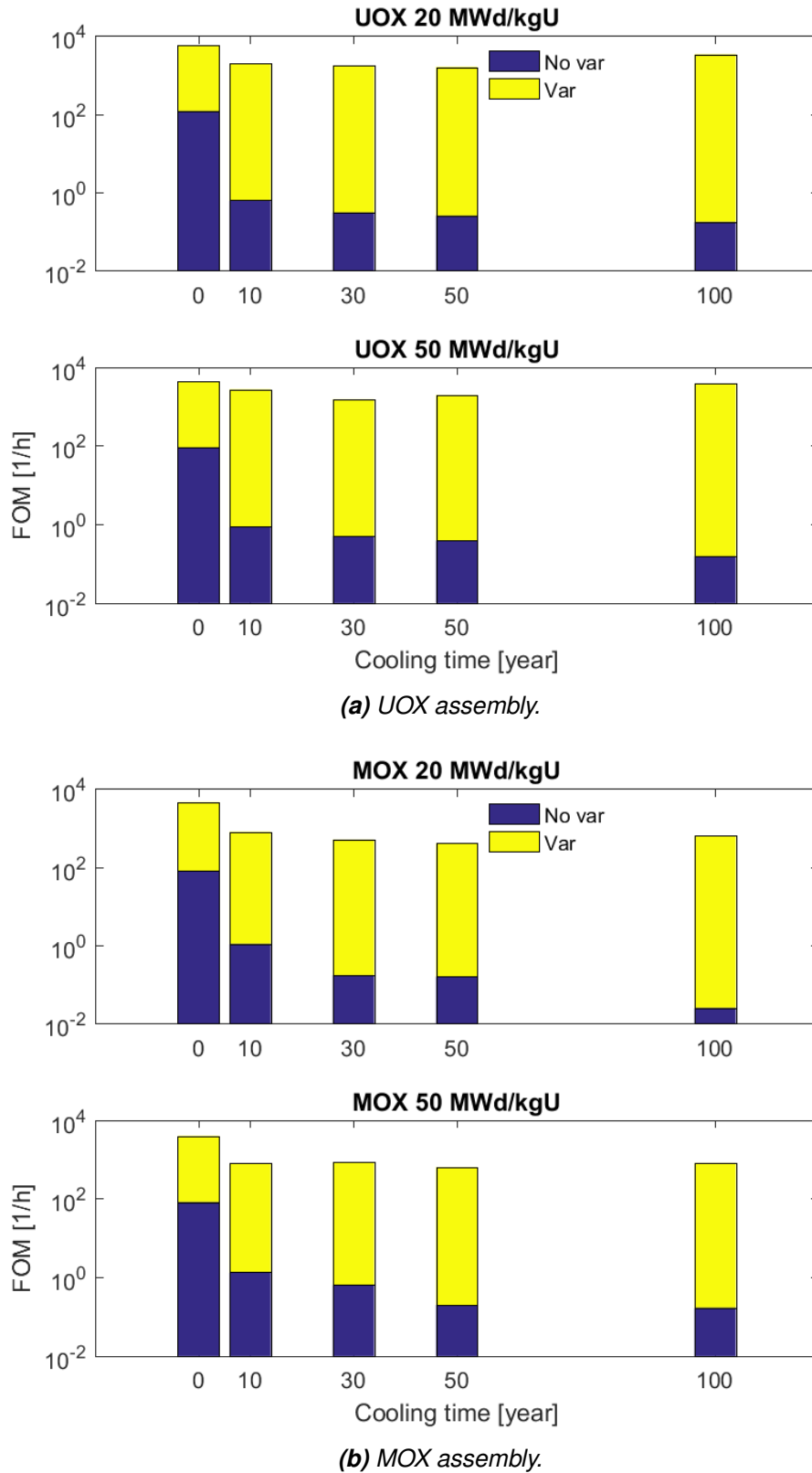


**Figure 4.** Figure of merit in photon dose rate calculations. The vertical axis is in logarithmic scale. Blue colour indicates a calculation without variance reduction and yellow with variance reduction.

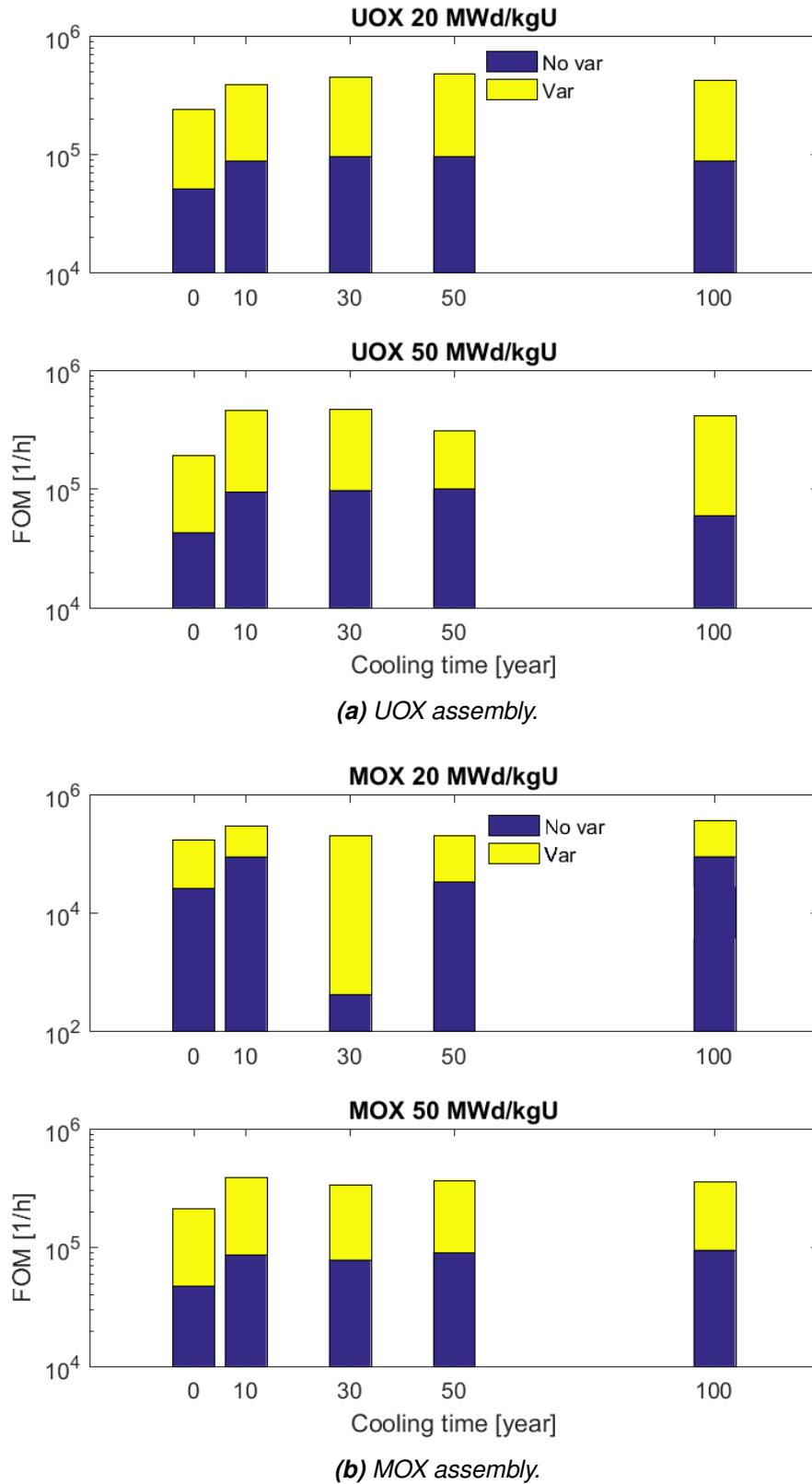


**Figure 5.** Figure of merit in neutron flux calculations. The vertical axis is in logarithmic scale. Blue colour indicates a calculation without variance reduction and yellow with variance reduction.